Design of Multistage Extractive Reaction Processes

Ketan D. Samant and Ka M. Ng
Dept. of Chemical Engineering, University of Massachusetts, Amherst, MA 01003

Multistage extractive reaction (MSER) processes can successfully improve the yield of and selectivity to the desired product, as well as separation of byproducts. A general and efficient design procedure for stand-alone countercurrent MSER cascades and process flowsheets presented here determines the range of feasible operation for the MSER process, the number of stages in the MSER cascade, compositions and molar flow rates at each stage, and the yield or product distribution of the reaction system. It is based on the geometric properties of the phase and reaction equilibrium surfaces and the composition profiles of the MSER cascade. First, a key design variable is identified and the fixed points or pinches of the composition profiles are tracked as a function of this variable by using arc-length continuation, without performing stage-to-stage calculations. The location of the fixed points gives the upper or lower bound on the window of the MSER operation. The other bound is determined by the equilibrium behavior of the system. Within the window of operation MSER profiles are guaranteed to be feasible. Then, stage-to-stage calculations are performed as an initial-value problem to complete the design. The results of these calculations provide a comprehensive picture of the trade-offs in the design of MSER processes and can be used as a basis for screening flowsheet alternatives. The procedure is illustrated with several design examples.

Introduction

Reactive separation processes have received considerable attention in recent years as alternatives to conventional processes. Simultaneous reaction and separation offers certain advantages that cannot be matched by conventional processes, for example, reduced capital investment and freedom from reaction equilibrium limitations. The use of reactive distillation in the production of methyl acetate and methyl-tertbutyl ether clearly demonstrates some of the benefits (DeGarmo et al., 1992; Doherty and Buzad, 1992). Processes involving simultaneous reaction and adsorption in a chromatographic reactor (Coca et al., 1993; Tonkovich and Carr, 1994), permeation in a membrane reactor (Tsotsis et al., 1993), crystallization (Berry and Ng, 1997; Mersmann and Kind, 1988), and extraction in a liquid–liquid two-phase reactor (Sharma, 1988; Samant and Ng, 1998a) offer similar advantages. The last process, extractive reaction, involves simultaneous reaction and liquid–liquid phase separation. The immiscibility may occur naturally with the reaction under consideration or may be deliberately introduced by addition of solvent(s). Examples of applications of extractive reaction processes can be found in the literature (Anderson and Veysoglu, 1973; King et al., 1985; Chapman, 1987; Kuntz, 1987; Pahari and Sharma, 1991).

Extractive reaction processes have the potential of providing significant improvements in yield of the desired product, selectivity to the desired product, and ease of separation of byproducts. In some cases, they also offer the advantage of a reduction in the amount of process equipment by combining the reaction and extraction operations into one single unit. However, extractive reaction processes may not always be beneficial. In some cases, the operation may not be feasible except at prohibitively high solvent flow rates. In other cases, the improvements obtained over conventional single-phase processes in the feasible range of operation may not be significant enough to justify the use of extractive reactions. Hence, for successful development of these processes, it is essential to have a procedure to synthesize process flow-

Correspondence concerning this article should be addressed to K. M. Ng.

sheets and to analyze them to see if they indeed meet the desired objectives. The procedure for synthesis of flowsheets for extractive reaction processes is discussed by Samant and Ng (1998a). It was pointed out that the use of MSERs for systems with one or more than one degree of freedom at thermodynamic equilibrium at constant temperature and pressure can lead to improvements in process performance. The intent of this article is to extend this synthesis procedure to analysis of the flowsheets developed. Specifically, we develop and present an efficient and general method for design of MSER processes. Equilibrium thermodynamic analysis forms the basis of this method. The method identifies the key design variables for the process, determines the ranges of these variables for feasible operation, and evaluates the process trade-offs within this range. It can be used as a tool for screening process alternatives and for comparing extractive reaction processes against conventional processes.

Classic methods for the design of extractors involve graphical techniques and are restricted to nonreactive ternary systems (Treybal, 1981). A more general geometric method for design of extractors for nonreactive multicomponent systems was presented by Minotti et al. (1996). Our procedure is applicable to the general case of multicomponent extractive reactions for designing stand-alone MSER cascades as well as MSER process flowsheets.

The method is illustrated with two examples. One considers a four-component system for improvement in yield of the desired product. The other considers a five-component system involving reactions in series or in parallel; it demonstrates the improvement in the selectivity to the desired product. The design of a stand-alone unit and the entire flowsheet is considered for both cases. These examples are hypothetical but general. Any real system can be analyzed similarly with relevant data.

Design of Multistage Extractive Reactors

Transformed mole fraction coordinates

The method for design of multistage extractive reactors is based on analysis of the phase behavior of multicomponent, multireaction systems at thermodynamic equilibrium. When we analyze the phase behavior, it is highly desirable to be able to visualize it. In mole fraction coordinates, however, we cannot plot even isothermal, isobaric phase diagrams for systems with more than four components without having to resort to a number of cuts and projections. To eliminate this restriction on visualization of phase diagrams, Ung and Doherty (1995a) introduced transformed mole fraction coordinates as discussed below.

Consider a multicomponent system of c components undergoing r chemical reactions. The r reactions can be represented as

$$\nu_{1,m}A_1 + \nu_{2,m}A_2 + \cdots + \nu_{c,m}A_c = 0 \qquad m = 1, 2, \ldots, r, \quad (1)$$

where A_i are the reacting species and $\nu_{i,m}$ is the stoichiometric coefficient of component i in reaction m. By convention, $\nu_{i,m} < 0$ if component i is a reactant in reaction m; $\nu_{i,m} > 0$ if component i is a product of reaction m; and $\nu_{i,m} = 0$ if it does not take part in reaction m. Using vector–matrix formalism, we define:

$$\nu_i^T = (\nu_{i,1}, \nu_{i,2}, \ldots, \nu_{i,r}) \quad (2)$$

$$\nu_{\mathrm{TOT}}^T = (\nu_{\mathrm{TOT},1}, \nu_{\mathrm{TOT},2}, \ldots, \nu_{\mathrm{TOT},r}), \quad (3)$$

where ν_i^T is the row vector of stoichiometric coefficients of component i in each reaction, and ν_{TOT}^T is the row vector of the sum of the stoichiometric coefficients for each reaction. We choose r reference components and define:

$$\boldsymbol{x}_{\mathrm{Ref}} = (x_{(c-r+1)}, x_{(c-r+2)}, \ldots, x_c)^T \quad (4)$$

$$\boldsymbol{V} = \begin{Bmatrix} \nu_{(c-r+1),1} & \cdots & \nu_{(c-r+1),r} \\ \cdots & \nu_{i,r} & \cdots \\ \nu_{c,1} & \cdots & \nu_{c,r} \end{Bmatrix}, \quad (5)$$

where $\boldsymbol{x}_{\mathrm{Ref}}$ is the column vector composed of the mole fractions of the r reference components, and $\boldsymbol{V}$ is the square matrix of stoichiometric coefficients for the r reference components in the r reactions. We choose r reference components, as we can reduce the dimensionality of the system by r (the number of reactions). Reference components are chosen such that the matrix $\boldsymbol{V}$ is nonsingular. Following the developments of Ung and Doherty (1995a), the transformed mole fraction coordinates are defined as

$$X_i = \frac{x_i - \nu_i^T \boldsymbol{V}^{-1} \boldsymbol{x}_{\mathrm{Ref}}}{1 - \nu_{\mathrm{TOT}}^T \boldsymbol{V}^{-1} \boldsymbol{x}_{\mathrm{Ref}}} \qquad i = 1, 2, \ldots, c-r. \quad (6)$$

The transformed mole fractions as just defined add up to unity and are reaction invariant:

$$\sum_{i=1}^{c-r} X_i = 1 \quad (7)$$

$$X_i(0) = X_i(\underline{\xi}) \qquad \forall \underline{\xi} \qquad i = 1, 2, \ldots, c-r, \quad (8)$$

where $\underline{\xi}$ is the column vector of the r dimensionless extents of reaction:

$$\underline{\xi} = (\xi_1, \xi_2, \ldots, \xi_r)^T. \quad (9)$$

Thus, provided that $c - r \leq 4$, isothermal, isobaric phase diagrams of systems with any number of components and reactions can be plotted on paper for visualization. In essence, a reactive phase diagram in transformed coordinate space is a projection/transformation of the reaction equilibrium surface (or intersection of reaction equilibrium surfaces in the case of multiple reactions) onto a lower-dimensional coordinate system. Every composition on this diagram satisfies the reaction equilibrium equations. Liquid–liquid phase splits are shown on the reactive phase diagram with a "reactive" phase envelope. It represents the projection of the intersection of phase and reaction equilibrium surfaces onto the transformed coordinate system. Every composition on a reactive phase envelope satisfies phase and reaction equilibrium equations. These transforms have been used by a number of researchers for different reactive separation processes, such as reactive distillation (Ung and Doherty, 1995b), reactive

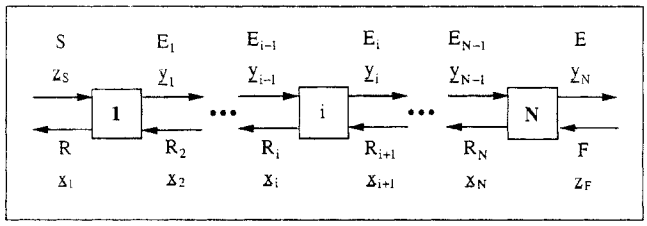

Figure 1. Countercurrent multistage extractive reactor (MSER) cascade.

Streams leaving each stage are in phase and reaction equilibrium.

crystallization (Berry and Ng, 1997), and extractive reactions (Samant and Ng, 1998a).

Extractive reactor model

The MSER model is shown in Figure 1. The MSER cascade comprises a solvent-rich extract stream and a solvent-lean raffinate stream in countercurrent flow. We assume that the cascade operates at constant temperature and pressure. This assumption can easily be relaxed if temperatures and pressures on each stage of the cascade are specified. The liquid phases leaving each stage are in phase and reaction equilibrium.

Consider an MSER with a feed stream composed of z_F and molar flow rate F, a solvent stream composed of z_S and molar flow rate S, an extract stream composed of y_N and molar flow rate E, and a raffinate stream composed of x_1 and molar flow rate R, where

$$z_F = (z_{1F}, z_{2F}, \ldots, z_{cF})^T \tag{10}$$

$$z_S = (z_{1S}, z_{2S}, \ldots, z_{cS})^T \tag{11}$$

$$y_N = (y_{1N}, y_{2N}, \ldots, y_{cN})^T \tag{12}$$

$$x_1 = (x_{11}, x_{21}, \ldots, x_{c1})^T \tag{13}$$

The material balance around the MSER gives

$$Fz_{iF} + Sz_{iS} + Ey_{iN} + Rx_{i1} - \nu_i^T \underline{\epsilon} \quad i = 1, 2, \ldots, c, \tag{14}$$

where $\underline{\epsilon}$ is the column vector of the r molar extents of reaction

$$\underline{\epsilon} = (\epsilon_1, \epsilon_2, \ldots, \epsilon_r)^T. \tag{15}$$

Using the r reference components we can split Eq. 14 as

$$Fz_{\mathrm{Ref},F} + Sz_{\mathrm{Ref},S} = Ey_{\mathrm{Ref},N} + Rx_{\mathrm{Ref},1} - V\underline{\epsilon} \tag{16}$$

$$Fz_{iF} + Sz_{iS} = Ey_{iN} + Rx_{i1} - \nu_i^T \underline{\epsilon} \quad i = 1, 2, \ldots, c-r-1 \tag{17}$$

$$F + S = E + R - \nu_{\mathrm{TOT}}^T \underline{\epsilon} \tag{18}$$

where

$$z_{\mathrm{Ref},F} = (z_{(c-r+1)F}, \ldots, z_{cF})^T \tag{19}$$

$$z_{\mathrm{Ref},S} = (z_{(c-r+1)S}, \ldots, z_{cS})^T \tag{20}$$

$$y_{\mathrm{Ref},N} = (y_{(c-r+1)N}, \ldots, y_{cN})^T \tag{21}$$

$$x_{\mathrm{Ref},1} = (x_{(c-r+1)1}, \ldots, x_{c1})^T. \tag{22}$$

We now eliminate $\underline{\epsilon}$ from Eqs. 17 and 18 by using Eq. 16 to get

$$F\left(z_{iF} - \nu_i^T V^{-1} z_{\mathrm{Ref},F}\right) + S\left(z_{iS} - \nu_i^T V^{-1} z_{\mathrm{Ref},S}\right) = E\left(y_{iN} - \nu_i^T V^{-1} y_{\mathrm{Ref},N}\right) + R\left(x_{i1} - \nu_i^T V^{-1} x_{\mathrm{Ref},1}\right) \quad i = 1, 2, \ldots, c-r-1 \tag{23}$$

$$F\left(1 - \nu_{\mathrm{TOT}}^T V^{-1} z_{\mathrm{Ref},F}\right) + S\left(1 - \nu_{\mathrm{TOT}}^T V^{-1} z_{\mathrm{Ref},S}\right) = E\left(1 - \nu_{\mathrm{TOT}}^T V^{-1} y_{\mathrm{Ref},N}\right) + R\left(1 - \nu_{\mathrm{TOT}}^T V^{-1} x_{\mathrm{Ref},1}\right). \tag{24}$$

We define transformed molar flow rates for the feed, solvent, extract, and raffinate streams as

$$\hat{F} = F\left(1 - \nu_{\mathrm{TOT}}^T V^{-1} z_{\mathrm{Ref},F}\right) \tag{25}$$

$$\hat{S} = S\left(1 - \nu_{\mathrm{TOT}}^T V^{-1} z_{\mathrm{Ref},S}\right) \tag{26}$$

$$\hat{E} = E\left(1 - \nu_{\mathrm{TOT}}^T V^{-1} y_{\mathrm{Ref},N}\right) \tag{27}$$

$$\hat{R} = R\left(1 - \nu_{\mathrm{TOT}}^T V^{-1} x_{\mathrm{Ref},1}\right) \tag{28}$$

and write Eqs. 23 and 24 as

$$\hat{F}Z_{iF} + \hat{S}Z_{iS} = \hat{E}Y_{iN} + \hat{R}X_{i1} \quad i = 1, 2, \ldots, c-r-1 \tag{29}$$

$$\hat{F} + \hat{S} = \hat{E} + \hat{R}, \tag{30}$$

where Z_{iF}, Z_{iS}, Y_{iN}, and X_{i1} are the transformed mole fractions of component i in the feed, solvent, extract, and raffinate streams, respectively; defined by the general definition given in Eq. 6. We can combine Eqs. 29 and 30 using vector notation to write the overall material balance equation as

$$\hat{F}\mathbf{Z}_F + \hat{S}\mathbf{Z}_S = \hat{E}\mathbf{Y}_N + \hat{R}\mathbf{X}_1, \tag{31}$$

where $\mathbf{Z}_F$, $\mathbf{Z}_S$, $\mathbf{Y}_N$, and $\mathbf{X}_1$ are the column vectors of $c-r$ transformed mole fractions of the feed, solvent, extract, and raffinate streams, respectively.

Following the same developments, we can write the material balance equations for each stage within the cascade as

$$\hat{E}_{i-1}\mathbf{Y}_{i-1} + \hat{R}_{i+1}\mathbf{X}_{i+1} = \hat{E}_i\mathbf{Y}_i + \hat{R}_i\mathbf{X}_i \quad i = 1, 2, \ldots, N, \tag{32}$$

where $\mathbf{Y}_i$ and $\mathbf{X}_i$ are the transformed composition vectors for the extract and raffinate phases leaving stage i, and $\hat{E}_i$ and $\hat{R}_i$ are the corresponding transformed flow rates (here $\hat{R}_1 = \hat{R}$, $\hat{E}_N = \hat{E}$, $\hat{E}_0 = \hat{S}$, $\mathbf{Y}_0 = \mathbf{Z}_S$, $\hat{R}_{N+1} = \hat{F}$, and $\mathbf{X}_{N+1} = \mathbf{Z}_F$). It should be noted that the overall material balance given by Eq. 31 is equivalent to the sum of N stage balance equations

given by Eq. 32. Also, the streams leaving any stage i are in phase and reaction equilibrium.

$$\boldsymbol{Y}_i = f_{\text{eq}}(\boldsymbol{X}_i) \qquad i = 1, 2, \ldots, N. \tag{33}$$

The vector function f_{eq} represents the set of c phase equilibrium and r reaction equilibrium equations.

In addition, the mole fractions and the transformed mole fractions of each stream in the cascade should sum up to unity.

$$\sum_{k=1}^{c} y_{ki} = \sum_{k=1}^{c-r} Y_{ki} = 1.0 \qquad i = 0, 1, \ldots, N \tag{34}$$

$$\sum_{k=1}^{c} x_{ki} = \sum_{k=1}^{c-r} X_{ki} = 1.0 \qquad i = 1, 2, \ldots, N+1. \tag{35}$$

The design problem and degrees of freedom

Equations 31 to 35 completely describe the design problem, which includes determination of the number of stages in the MSER cascade, the composition profile, the molar flow rates, and yield or product distribution for the reaction system under consideration. The number of independent variables for the design problem is obtained from a degrees-of-freedom analysis. At each of the N stages, there are $(c-r)$ independent material balance equations given by Eq. 32 and $(c+r)$ independent equilibrium equations given by Eq. 33. There are $2(N+1)$ additional equations given by Eqs. 34 and 35, thus giving a total of $2cN+2(N+1)$ equations. These equations can also be written in terms of mole fractions instead of transformed mole fractions, as the functional relationships between mole fractions and transformed mole fractions and molar flow rates and transformed molar flow rates are known (Eqs. 6, 25–28). The variables are N, S, z_S, F, z_F, and E_i, $\boldsymbol{y}_i$, R_i, $\boldsymbol{x}_i$ for $i = 1, 2, \ldots, N$. Each composition vector consists of c mole fractions. Thus we have $2c(N+1)+2(N+1)+1$ variables. Therefore, the design problem has $(2c+1)$ degrees of freedom. S, z_S, F, and z_F are often specified. The feed and the solvent streams have only $(c-1)$ independent mole fractions. Hence these specifications account for $(2c)$ degrees of freedom. The remaining degree of freedom is specified by choosing a mole fraction of any species j in the raffinate phase (x_{j1} or X_{j1}). In principle, the design problem can be completely solved with these $(2c+1)$ specifications.

To obtain the number of stages and the MSER composition profile (operating line), we have to solve Eqs. 32 to 35 at each stage for the unknown flow rates and compositions. This is an initial-value problem whose solution is started from stage 1 (or alternatively from stage N). To determine the unknown flow rates and compositions at the first stage, we need to solve the following equations:

$$\hat{S}\boldsymbol{Z}_S + \hat{R}_2\boldsymbol{X}_2 = \hat{E}_1\boldsymbol{Y}_1 + \hat{R}_1\boldsymbol{X}_1 \tag{36}$$

$$\boldsymbol{Y}_1 = f_{\text{eq}}(\boldsymbol{X}_1) \tag{37}$$

$$\boldsymbol{Y}_2 = f_{\text{eq}}(\boldsymbol{X}_2) \tag{38}$$

$$\sum_{i=1}^{c-r} Z_{iS} = \sum_{i=1}^{c-r} X_{i1} = \sum_{i=1}^{c-r} X_{i2} = \sum_{i=1}^{c-r} Y_{i1} = \sum_{i=1}^{c-r} Y_{i2} = 1.0. \tag{39}$$

Equation 36 represents $(c-r)$ material balance equations on stage 1. Equations 37 and 38 indicate that streams leaving stages 1 and 2 are in phase and reaction equilibrium and form a set of $2(c+r)$ equations. Although stream E_2 does not appear in the material balance equations, we include the composition of this stream in our equations, as this stream is in phase and reaction equilibrium with stream R_2, which enters stage 1. There are five additional equations given by Eq. 39. Hence at the first stage of the initial-value problem, we have $(3c+r+5)$ equations. In these equations we have a total of $(5c+4)$ variables, which are S, z_S, R_1, $\boldsymbol{x}_1$, R_2, $\boldsymbol{x}_2$, E_1, $\boldsymbol{y}_1$, and $\boldsymbol{y}_2$. Hence, we have $(2c-r-1)$ degrees of freedom. As mentioned previously, S, z_S, and $\boldsymbol{X}_{j1}$ (or x_{j1}), a total of $(c+1)$ variables, are already specified for the design problem. Hence, to initiate the solution of the initial-value problem we need to calculate $(c-r-2)$ variables.

The only way this can be done is by solving the overall material balance (Eq. 31), as this is the only equation that contains additional information in the form of F and z_F. The overall balance has $(c-r)$ independent equations. The variables are S, z_S, F, z_F, E, $\boldsymbol{y}_N$, R, and $\boldsymbol{x}_1$. The outlet extract and raffinate compositions must satisfy phase and reaction equilibrium equations. Therefore, by Gibbs' phase rule at constant temperature and pressure, the composition vectors $\boldsymbol{y}_N$ and $\boldsymbol{x}_1$ each have $(c-r-2)$ independent mole fractions. Thus we have a total of $2(c-1)+2(c-r-2)+4$ variables, $(c-r)$ equations, and $(3c-r-2)$ degrees of freedom for the overall balance. We can solve the overall balance and start the solution of the initial-value problem without any additional information only if the degrees of freedom for the design problem and the overall balance are equal, that is,

$$c - r = 3. \tag{40}$$

To solve the overall balance equation and the initial-value problem for systems where $c-r>3$, we have to assume $(c-r-3)$ variables in addition to the $(2c+1)$ design specifications. These $(c-r-3)$ variables are updated iteratively until a solution that satisfies Eqs. 31 to 35 is obtained. In this article we consider examples that satisfy Eq. 40. It should be noted that the condition given by Eq. 40 for a nonreacting system is $c=3$. The presence of reaction(s) allows us to handle, without iterations, systems with more than three components.

Feasibility of operation

The design problem is completely defined by specifying S (or S/F), z_S, F, z_F, and X_{j1}, and this information is adequate to solve the initial-value problem for systems that satisfy Eq. 40. However, this information alone does not guarantee feasibility of operation. MSER operation is feasible only for certain values of solvent flow rate, S/F. For feasible operation, the compositions of the raffinate streams $\boldsymbol{X}_i$ $(i = 1, 2, \ldots, N)$ should lie on the solvent-lean side, and the compositions of the extract streams $\boldsymbol{Y}_i$ $(i = 1, 2, \ldots, N)$ should lie on the solvent-rich side of the reactive phase equilibrium surface. For a system with c components and r reactions, the

reactive phase equilibrium surface is a $(c-r-2)$-dimensional surface corresponding to the intersection of phase and reaction equilibrium surfaces. When S, z_S, F, z_F, and X_{j1} are specified, the preceding requirement is met only for a certain range of solvent flow rates $S/F \in [(S/F)_{\text{lower}}, (S/F)_{\text{upper}}]$. This is the range of operation of the MSER for the specified design variables. In general, the upper and lower bounds on the range of operation are governed by the equilibrium behavior of the system under consideration. Determination of these bounds for specific cases of interest is demonstrated in Examples 1 and 2.

Feasible operation is not guaranteed for all values of S/F within these bounds. Typically, as in the case of nonreacting systems, we should expect a minimum value of S/F. For $(S/F)_{\text{upper}} \geq (S/F) > (S/F)_{\text{min}}$, the profile should attain the extract target composition y_N in a finite number of stages. For $(S/F)_{\text{lower}} \leq (S/F) \leq (S/F)_{\text{min}}$, the profile should not attain the target composition even in an infinite number of stages, and the equilibrium and operating curves should touch or intersect (pinch) at one or more points. We should ensure the feasibility of operation by determining the value of $(S/F)_{\text{min}}$ before trying to evaluate the equilibrium stage requirements and the process trade-offs. This problem of determination of the minimum solvent flow is discussed in the following subsection.

Estimation of minimum solvent flow

For systems that satisfy the constraint of Eq. 40, the minimum solvent flow requirement can be determined by tracking the fixed points of the MSER model equations, that is, by tracking the points of intersection of the equilibrium and operating curves. This approach eliminates the need to perform stage-to-stage calculations at each and every value of S/F. All values of S/F within the MSER range of operation for which fixed points exist are calculated. The highest value of S/F for which a fixed point exists corresponds to the minimum solvent flow $(S/F)_{\text{min}}$. This technique was also used by Minotti et al. (1996) for nonreactive systems.

At a fixed point (pinch) in the MSER profile, the equilibrium curve and the operating curve touch or intersect. The stream compositions do not change from stage to stage. If a pinch exists at the kth stage, then

$$\boldsymbol{X}_k = \boldsymbol{X}_{k+1} = \cdots = \boldsymbol{X}_N = \hat{\boldsymbol{X}} \tag{41}$$

$$\boldsymbol{Y}_{k-1} = \boldsymbol{Y}_k = \cdots = \boldsymbol{Y}_N = \hat{\boldsymbol{Y}} \tag{42}$$

$$\hat{\boldsymbol{Y}} = f_{\text{eq}}(\hat{\boldsymbol{X}}). \tag{43}$$

Hence the fixed points of the MSER profile will satisfy Eq. 43 and the following material balance equations

$$\hat{S}\boldsymbol{Z}_S - \hat{R}\boldsymbol{X}_1 = \hat{E}_p\hat{\boldsymbol{Y}} - \hat{R}_p\hat{\boldsymbol{X}} \tag{44}$$

$$\hat{S}\boldsymbol{Z}_S + \hat{F}\boldsymbol{Z}_F = \hat{E}_N\boldsymbol{Y}_N + \hat{R}\boldsymbol{X}_1, \tag{45}$$

where $\hat{E}_p$ and $\hat{R}_p$ are the transformed molar flow rates of the extract and the raffinate streams at the pinch. Equations 44 and 45 can be written in the form of a vector function $\boldsymbol{F}$ as:

$$\boldsymbol{F}\left(\hat{\boldsymbol{X}}, \boldsymbol{Y}_N, \hat{E}_p, \hat{R}_p, \hat{E}_N, \hat{R}, S/F\right) = 0. \tag{46}$$

This equation represents a set of $(c-r)$ material balance equations at the pinch (Eq. 44) and $(c-r)$ overall balance equations (Eq. 45). We have used the design specifications z_S, F, z_F, and X_{j1} and Eq. 43 to eliminate the remaining variables from Eqs. 44 and 45.

Equation 46 is solved by using a parametric continuation method. The branch of solutions of Eq. 46 is tracked, starting at a known solution, by using $\lambda = S/F$ as a continuation parameter. The parameter continuation may be written as

$$\boldsymbol{F}\left(\hat{\boldsymbol{X}}, \boldsymbol{Y}_N, \hat{E}_p, \hat{R}_p, \hat{E}_N, \hat{R}; \lambda\right) = 0. \tag{47}$$

The parameter continuation of this form fails when there exists a turning (limit) point in the $\hat{\boldsymbol{X}}$ vs. λ graph, as at this point the Jacobian of $\boldsymbol{F}$ becomes singular (Seader, 1985). At this point, the equilibrium and operating curves are tangent to each other (tangent pinch). This difficulty is eliminated by using a pseudo-arc-length continuation technique, which chooses any one of the variables as the continuation parameter (Kubicek, 1976). The solution to Eq. 47 at the Nth stage (feed pinch), $\hat{\boldsymbol{X}}_F = \boldsymbol{X}_N$, $(\boldsymbol{Y}_{N-1} = \boldsymbol{Y}_N = \hat{\boldsymbol{Y}}_F = f_{\text{eq}}(\hat{\boldsymbol{X}}_F))$, is used as the starting point for the continuation method. The feed pinch solution can easily be calculated by using Newton's method.

Some solutions obtained by this method are not physically meaningful. Therefore, we impose the following constraints on the solutions:

$$\|\hat{\boldsymbol{X}}\| \geq \|\boldsymbol{X}_1\| \tag{48}$$

$$\|\hat{\boldsymbol{Y}}\| \leq \|\boldsymbol{Y}_N\|. \tag{49}$$

The norms of the transformed composition vectors depend on the equilibrium behavior of the system. The form of these constraints for specific cases of interest (Examples 1 and 2) is considered in the following sections. The fixed point that controls the minimum solvent flow, that is, which corresponds to the highest value of S/F, will occur either at $\hat{\boldsymbol{X}} = \hat{\boldsymbol{X}}_F$ (feed pinch controlled) or at a turning point in the $\hat{\boldsymbol{X}}$ vs. λ graph (tangent pinch controlled).

In the following sections we present examples illustrating the fixed-point tracking technique and the design procedure.

Example 1: Improvement in Yield. Consider a system with the following reaction:

$$A \Leftrightarrow B + C. \tag{50}$$

A solvent I that is completely miscible with A and C but partially miscible with the desired product B can be used to improve the yield of B (Samant and Ng, 1998a), which is defined as follows:

$$\text{Yield} = \frac{\text{Amount of desired product produced}}{\text{Amount of reactant fed to the reactor}}. \tag{51}$$

Using A as the reference component, the transformed mole fractions for this system are:

$$X_B = \frac{x_B + x_A}{1 + x_A} \tag{52}$$

$$X_C = \frac{x_C + x_A}{1 + x_A} \tag{53}$$

$$X_I = \frac{x_I}{1 + x_A}. \tag{54}$$

Figure 2 shows the reactive phase diagram for this system. The parameters used to generate this diagram are listed in Table 1. Curve *rps* is the reactive phase envelope and the dashed lines represent reactive tie-lines. The region enclosed by the reactive phase envelope is the two-phase region. The feed, solvent, extract, and raffinate streams are also marked on the phase diagram. The design variables for the system are also specified in Table 1. For these specifications, the MSER range of operation is bounded by

$$\left(\frac{S}{F}\right)_{\text{lower}} = \left(\frac{\hat{S}}{\hat{F}}\right)_{\text{lower}} \frac{(1+z_{AF})}{(1+z_{AS})} = \frac{(Z_{iF} - X_{iL})}{(X_{iL} - Z_{iS})} \frac{(1+z_{AF})}{(1+z_{AS})}$$

$$i = B, C, I \tag{55}$$

$$\left(\frac{S}{F}\right)_{\text{upper}} = \left(\frac{\hat{S}}{\hat{F}}\right)_{\text{upper}} \frac{(1+z_{AF})}{(1+z_{AS})} = \frac{(Z_{iF} - X_{iU})}{(X_{iU} - Z_{iS})} \frac{(1+z_{AF})}{(1+z_{AS})}$$

$$i = B, C, I, \tag{56}$$

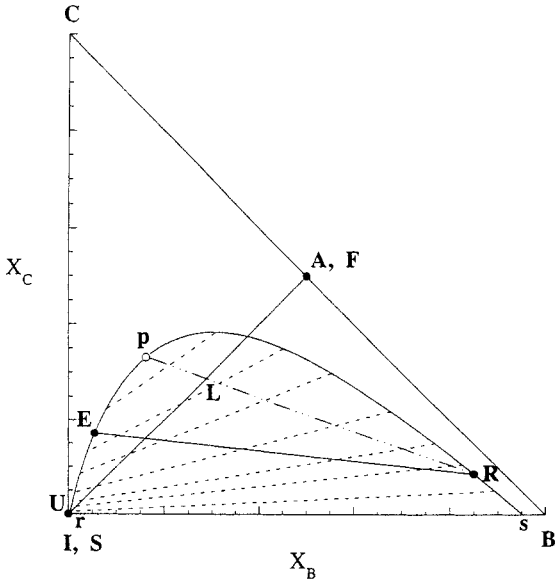

Figure 2. Reactive phase diagram for example 1.

The reactive phase diagram is plotted in transformed coordinate space to reduce the dimensionality of the system from three $(c-1)$ to two $(c-r-1)$. Every point on the reactive phase envelope (curve *rps*) is a projection of the intersection of the phase and reaction equilibrium surfaces in mole fraction coordinates.

Table 1. Thermodynamic Parameters and Design Specifications for Example 1

Temp. = 298.15 K; Pres. = 1 atm; Equil. const., $K = 2.0$		
UNIQUAC Equation Parameters (Sorenson and Arlt, 1979)		
Pure Component Parameters		
Component	r	q
A (4)	3.4543	3.052
B (3)	2.4088	2.248
C (2)	2.2024	2.072
I (1)	3.1878	2.400
Binary Interaction Parameters (K)		
a (1,1) = 0.0	a (1,2) = 41.146	a (1,3) = 649.05
a (2,1) = 56.488	a (2,2) = 0.0	a (2,3) = −229.71
a (3,1) = 113.53	a (3,2) = 121.11	a (3,3) = 0.0
a (4,1) = 17.119	a (4,2) = 157.6	a (4,3) = −25.154
	a (1,4) = 154.55	
	a (2,4) = −277.29	
	a (3,4) = 7.4068	
	a (4,4) = 0.0	
Design Specification		
$F = 1.0$		$X_{B1} = 0.75, 0.80, 0.85$
Component	z_{iF}	z_{iS}
A (4)	1.0	0.0
B (3)	0.0	0.0
C (2)	0.0	0.0
I (1)	0.0	1.0
Range of Operation		
$(S/F)_{\text{lower}} = 1.44$		$(S/F)_{\text{upper}} = 257.75$

where X_L and X_U are the transformed mole fractions at points L and U, respectively. The values of these bounds are listed in Table 1. Note that the first equality in Eqs. 55 and 56 follows from Eqs. 25 and 26, and the second equality results from the lever rule. Although not clearly visible on Figure 2, point U is the point of intersection of line SF and the reactive phase envelope *rps*. Solvent flow in excess of $(S/F)_{\text{upper}}$ will take us into the single-phase region of the reactive phase diagram. For solvent flow less than $(S/F)_{\text{lower}}$, it is no longer possible to obtain extract compositions on the solvent-rich side of the reactive phase envelope (i.e., curve *rp*).

For this system the constraints imposed by Eqs. 48 and 49 correspond to

$$\hat{X}_B \geq X_{B1} \tag{57}$$

$$\hat{Y}_B \leq Y_{BN}. \tag{58}$$

The first constraint states that the transformed mole fraction of B in the raffinate phase at the pinch cannot be less than that in the raffinate phase leaving stage 1 of the cascade, X_{B1} (a design variable). The second constraint expresses the fact that the transformed mole fraction of B in the extract phase at the pinch cannot be greater than that in the extract phase leaving stage N, Y_{BN} (which is determined by the overall material balance). These constraints can easily be derived from the phase diagram in Figure 2. The results of the fixed-point

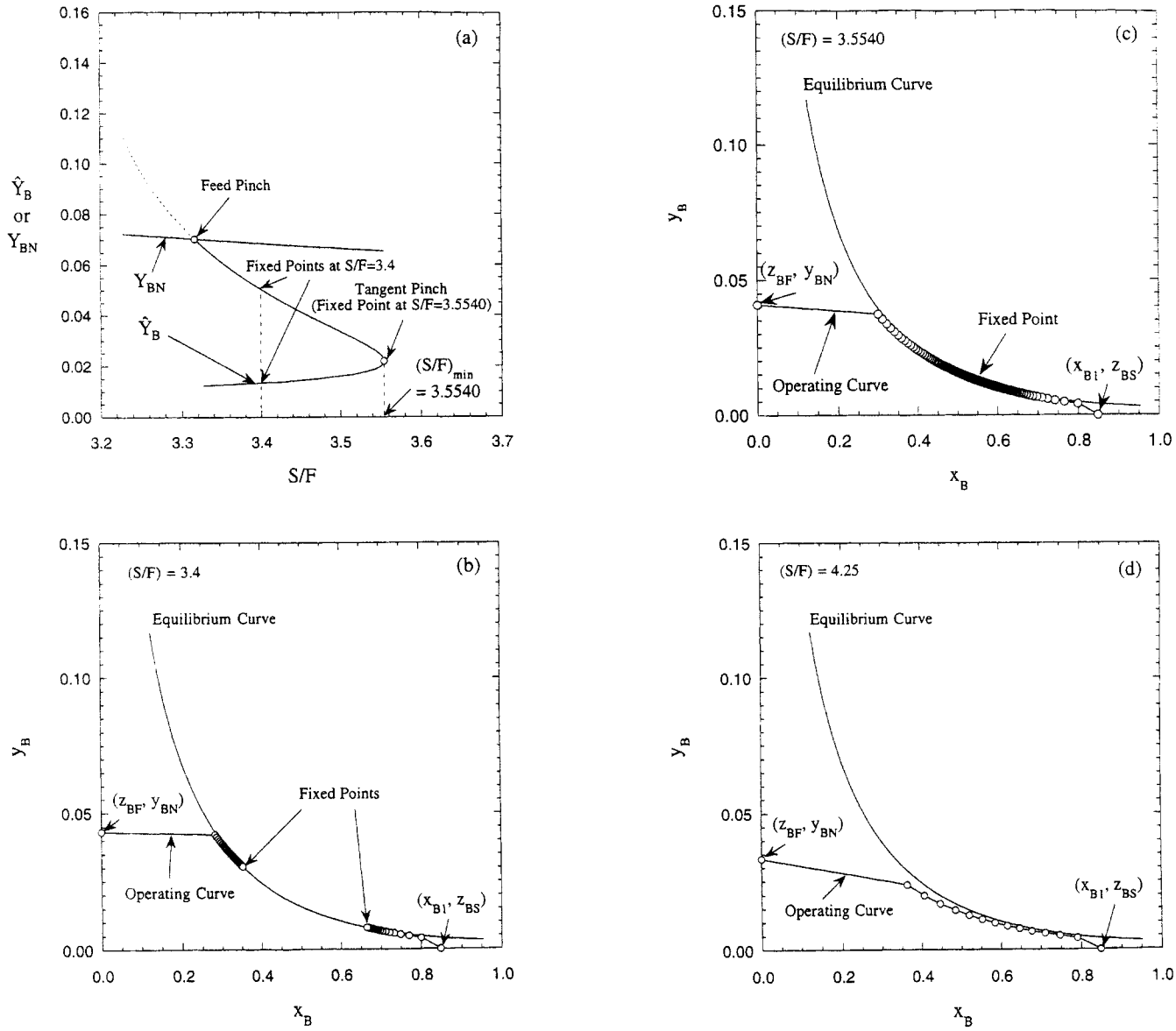

Figure 3. (a) Fixed points of the MSER profile as a function of S/F for example 1 ($X_{B1} = 0.85$); (b) extractor profile for $S/F = 3.4 < (S/F)_{min}$; (c) extractor profile for $S/F = 3.5540 = (S/F)_{min}$ (tangent pinch); (d) extractor profile for $S/F = 4.25 > (S/F)_{min}$ (feasible operation).

A tangent pinch is observed at $S/F = 3.5540$. MSER operation is feasible for solvent flow rates larger than 3.5540. Open circles indicate compositions of streams leaving each stage. According to the Gibbs phase rule, these streams have only 1 deg of freedom ($c - r - p$) at fixed T and P. Hence their compositions are completely specified just by specifying any 1 mole fraction (in this case, that of component B). Fixed points (pinches) are intersection points of operating and equilibrium curves.

tracking method (for $X_{B1} = 0.85$) are shown in Figure 3a. The curve $\hat{Y}_B$ vs. S/F represents the branch of fixed points of Eq. 47. The curve Y_{BN} vs. S/F represents the constraint imposed by Eq. 58. The branch of solutions above the feed pinch is shown by a dotted line and is ignored, as it violates this constraint. The branch of solutions shown by a solid line represents the solutions within the range of operation of the MSER. In this case, the fixed point that controls the minimum solvent flow requirement corresponds to the turning point. Hence, the system is tangent pinch controlled with $(S/F)_{min} = 3.5540$.

The MSER profiles for various values of S/F are shown in Figures 3b, 3c, and 3d. It should be noted that the profiles are plotted in mole fraction coordinates, as only one mole fraction is sufficient to specify the composition of a point on the reactive phase envelope. Figure 3b shows the profile for $S/F = 3.4$. For this value of S/F we have two fixed points within the range of operation (see Figure 3a). Hence, the equilibrium and operating curves intersect at two points and the target composition, (z_F, y_N), cannot be achieved even in an infinite number of stages. Figure 3c shows the profile at the tangent pinch ($S/F = 3.5540$). The equilibrium curve and

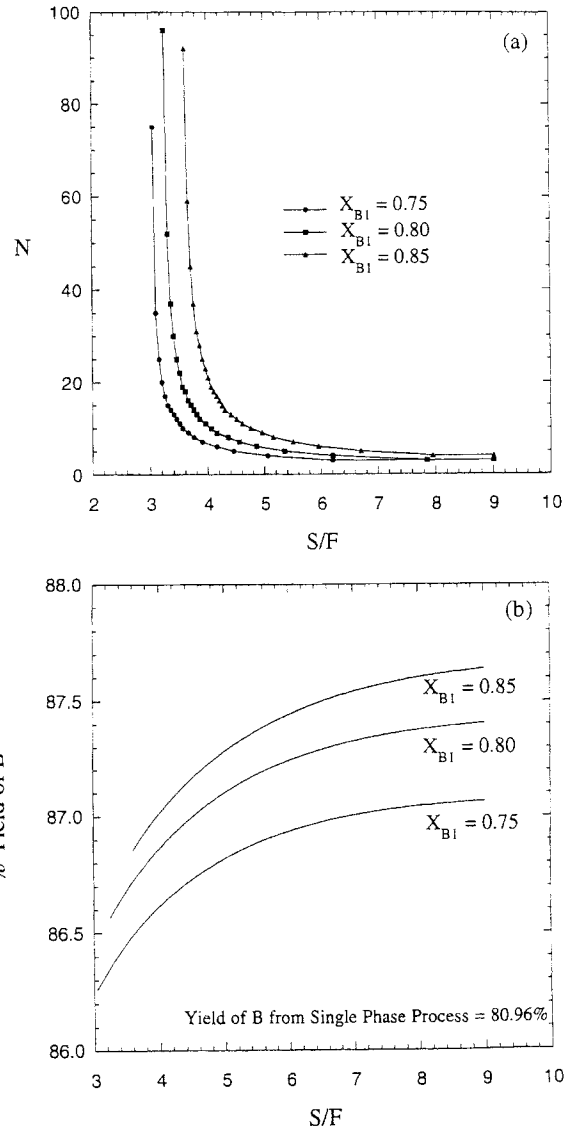

Figure 4. (a) Trade-off between S/F and equilibrium stage requirement for example 1; (b) yield of desired product as a function of S/F for example 1.

In part (a) the number of theoretical stages required increases sharply as minimum solvent flow is approached. As expected, part (b) shows that multistage extractive reaction gives significant improvement in yield over conventional single-phase processes.

the operating curve are tangent to each other at the fixed point and an infinite number of stages are required to achieve the target composition. The profile for $S/F = 4.25$ is shown in Figure 3d. This value of S/F is higher than the minimum, and hence the target composition is achieved in a finite number of stages.

Figure 4a shows the trade-off between the number of stages and solvent flow for different specifications of X_{B1}. The equilibrium stage requirement tends to infinity as the solvent flow rate approaches its minimum value. At the same S/F, the stage requirement decreases, as the outlet raffinate stream contains less desired product B. Also the minimum solvent flow $(S/F)_{min}$ requirement decreases, as the outlet raffinate contains less desired product. This should be contrasted with the yield vs. S/F plot in Figure 4b. The yield of the desired product at any S/F decreases with a decrease in the raffinate mole fraction of the desired product. However, the MSER cascade gives yields much higher than a single-phase process (0.8096) for all values of X_{B1}. It should also be noted that the yield increases with increasing solvent flow rate for all values of X_{B1}.

Example 2: Improvement in Selectivity. Consider a system with reactions in parallel:

$$A \leftrightarrow B + C$$
$$A \leftrightarrow D, \tag{59}$$

or with reactions in series

$$A \leftrightarrow B + C \leftrightarrow D. \tag{60}$$

Note that these two systems are equivalent at reaction equilibrium because of reversibility (see the Appendix). In both cases, the selectivity to the desired product B is parametrized by the product distribution as

$$\text{Product distribution} = \frac{\text{Total } B \text{ produced}}{\text{Total } A \text{ reacted}}. \tag{61}$$

The product distribution can be greatly improved by employing a solvent I that is miscible with A, C, and D, but that is partially miscible with B (Samant and Ng, 1998a). With A and D as reference components, the transformed mole fractions for this system are

$$X_B = \frac{x_B + x_A + x_D}{1 + x_A + x_D} \tag{62}$$

$$X_C = \frac{x_C + x_A + x_D}{1 + x_A + x_D} \tag{63}$$

$$X_I = \frac{x_I}{1 + x_A + x_D}. \tag{64}$$

Figure 5 shows the reactive phase diagram for this system. The thermodynamic parameters used for generating the reactive phase diagram are given in Table 2. The design variables used for the calculations are also listed in Table 2. The range of operation can be determined in a manner similar to the previous example and is listed in Table 2.

Figure 6 shows the branch of fixed points (for $X_{B1} = 0.85$) of Eq. 47 subject to the constraints of Eqs. 48 and 49. For this system, too, these constraints correspond to Eqs. 57 and 58. In this case, the fixed point that controls the minimum solvent flow corresponds to the feed pinch. Hence, the system is feed-pinch controlled with $(S/F)_{min} = 3.11$. A tangent pinch does not exist. For $S/F \leq 3.11$, the equilibrium and operating curves intersect at one point and for $S/F > 3.11$, they do not intersect, and thus the target composition is achieved in a finite number of stages.

The process trade-offs are shown in Figure 7. We observe from Figure 7a that the stage requirement tends to infinity as

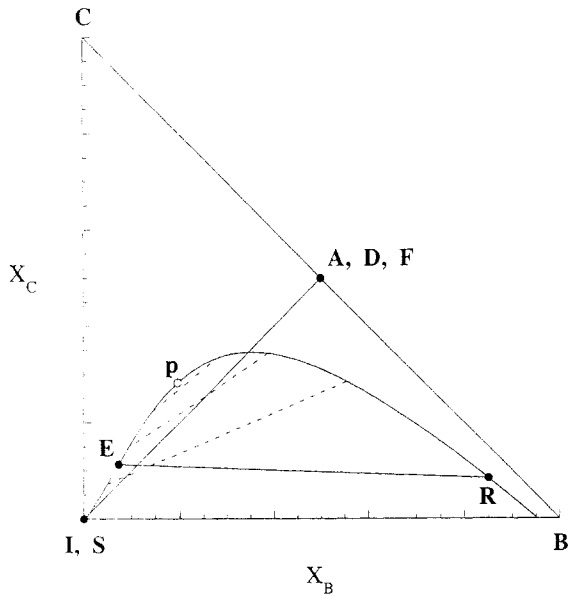

Figure 5. Reactive phase diagram for example 2.

The reactive phase diagram is plotted in transformed coordinate space to reduce the dimensionality of the system from four $(c-1)$ to two $(c-r-1)$. Every point on the reactive phase envelope (curve *rps*) is a projection of the intersection of the phase and reaction equilibrium surfaces in mole fraction coordinates.

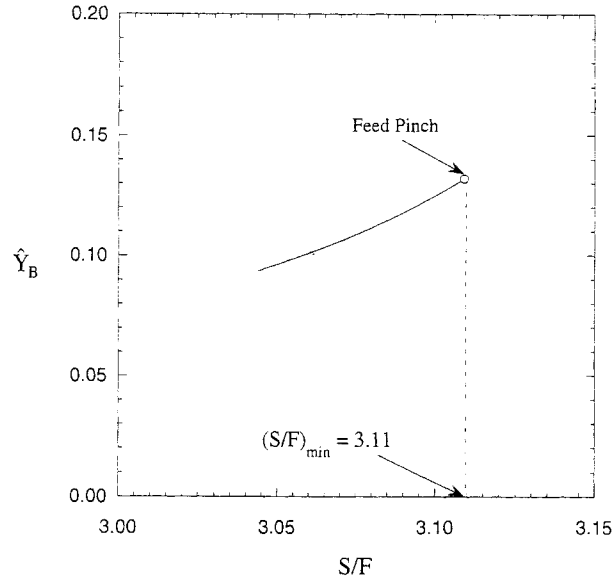

Figure 6. Fixed points of the MSER profile as a function of S/F for example 2 ($X_{B1} = 0.85$).

It shows a feed pinch. The target composition can be achieved with a normalized solvent flow rate (S/F) larger than 3.11.

Table 2. Thermodynamic Parameters and Design Specifications for Example 2

Temp. = 298.15 K; Pres. = 1 atm; Equil. const., $K_1 = 1.0$, $K_2 = K_3 = 2.0$		
UNIQUAC Equation Parameters (Sorenson and Arlt, 1979)		
Pure Component Parameters		
Component	r	q
A (4)	3.4543	3.052
B (1)	2.4088	2.248
C (2)	2.2024	2.072
D (5)	3.1680	2.484
I (3)	3.1878	2.400
Binary Interaction Parameters (K)		
a (1,1) = 0.0	a (1,2) = 121.11	a (1,3) = 113.53
a (2,1) = −229.71	a (2,2) = 0.0	a (2,3) = 56.488
a (3,1) = 649.05	a (3,2) = 41.146	a (3,3) = 0.0
a (4,1) = −25.154	a (4,2) = 157.60	a (4,3) = 17.119
a (5,1) = −209.39	a (5,2) = −485.54	a (5,3) = −99.271
a (1,4) = 7.4068	a (1,5) = 182.85	
a (2,4) = −277.29	a (2,5) = 436.64	
a (3,4) = 154.55	a (3,5) = 241.35	
a (4,4) = 0.0	a (4,5) = 298.52	
a (5,4) = 7.4239	a (5,5) = 0.0	
Design Specifications		
$F = 1.0$		$X_{B1} = 0.75, 0.80, 0.85$
Component	z_{iF}	z_{iS}
A (4)	1.0	0.0
B (1)	0.0	0.0
C (2)	0.0	0.0
D (5)	0.0	0.0
I (3)	0.0	1.0
Range of Operation		
$(S/F)_{lower} = 1.72$		$(S/F)_{upper} = 86.5$

the solvent flow approaches its minimum value. The stage requirement (at any given S/F) and $(S/F)_{min}$ decrease as X_{B1} decreases. However, the product distribution at a given S/F also decreases with decreasing X_{B1} (Figure 7b). The product distribution decreases with increasing S/F for all values of X_{B1}. However, the product distributions are vastly superior to that from a single-phase process (0.3824).

Design of MSER Process Flowsheets

In the preceding sections we presented with the aid of illustrations the method for design of an MSER cascade. For the problem of designing a stand-alone MSER cascade, the $(2c+1)$ degrees of freedom were specified by fixing S, z_S, F, z_F, and x_{j1} or X_{j1}. However, for the success of processes involving MSER cascades, it is essential to recover and recycle the solvent(s) and the unconverted reactant(s). The recycle streams, in general, will change the degrees of freedom of the process and we can no longer fix all of the just listed variables independently. However, the design technique for the stand-alone cascade can easily be adapted for the entire flow sheet. The design procedure involves the following steps:

1. Synthesize a process for the desired process objective(s), including improvement in yield, selectivity, and ease of separation (Samant and Ng, 1998a).
2. Determine the degrees of freedom of the process flowsheet.
3. Determine the window of operation of the MSER cascade.
4. Evaluate the process trade-offs within the window of operation.

The window of operation of the MSER cascade is the range of the key design variable for which the MSER operation is

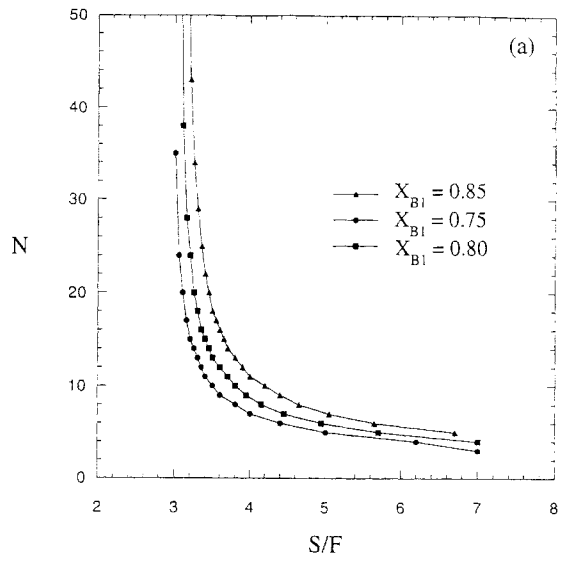

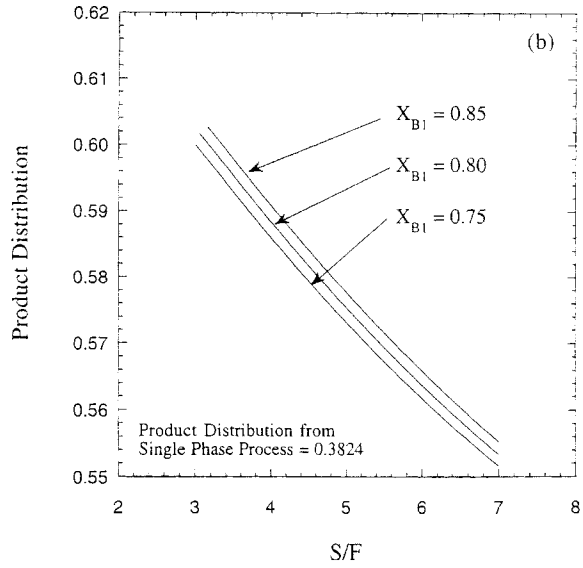

Figure 7. (a) Trade-off between S/F and equilibrium stage requirement for example 2; (b) product distribution as a function of S/F for example 2.

In part (a) the number of theoretical stages required increases sharply as minimum solvent flow is approached. Part (b) shows that the MSER process gives significant improvement in product distribution over conventional single-phase processes.

feasible. It should be noted that for the stand-alone MSER cascade, the key design variable is the solvent flow S/F and the window of operation corresponds to $(S/F)_{\text{upper}} \geq (S/F) > (S/F)_{\min}$. The design procedure is demonstrated with the following examples.

Example 3: Process for Improvement in Yield. A flowsheet for a process for improving the yield of desired product B of the system considered in Example 1 is shown in Figure 8. The flowsheet has three degrees of freedom if the compositions of feed and product streams and the degrees of separations in the separators are specified (Samant and Ng, 1998a). In this example and the next, we assume pure component feed and product streams and complete separation of the indicated component in the separators. The three degrees of freedom can be conveniently specified by fixing the raffinate flow rate, R, and the mole fraction of the desired product in the raffinate and the extract phases, X_{B1} and Y_{BN}. The flow rates and compositions of all streams are fixed once these degrees of freedom are specified.

In this analysis, we fix R and X_{B1} and determine the range of the key variable Y_{BN} for which the operation of MSER is feasible. This window of operation is obtained by reformulating the fixed-point tracking problem for the new key variable as follows.

If a fixed point, $(\hat{X}, \hat{Y})$, exists within the MSER range of operation for given values of R, X_{B1}, and Y_{BN}, it satisfies Eqs. 43, 44, and 45 and the constraints imposed by Eqs. 48 and 49. By eliminating the dependent variables, these equations can be written in the form of a vector function $\boldsymbol{G}$ as:

$$\boldsymbol{G}\left(\hat{X}_B, \hat{E}_p, \hat{R}_p; \lambda = Y_{BN}\right) = 0. \tag{65}$$

The vector function $\boldsymbol{G}$ represents a set of $(c-r)$ material balance equations at the fixed point. Note that the $(c-r)$ overall balance equations are already satisfied as S, z_S, F, z_F, E get fixed once R, X_{B1}, and Y_{BN} are specified. The pseudo-arc-length continuation technique is used to track the solutions of Eq. 65 subject to the constraints of Eqs. 48 and 49 with $\lambda = Y_{BN}$ as the continuation parameter. The feed-pinch solution is used as the starting point of the continuation method.

Figure 9 shows the branch of fixed points of the MSER profile for $X_{B1} = 0.85$. Note that this plot is independent of the value of R. This is because in Eq. 65, only $\hat{E}_p$ and $\hat{R}_p$ depend on R and $\hat{X}_B$ (and $\hat{Y}_B$) are independent of R. We observe that there exists a value of Y_{BN} below which the extractor profile does not have any fixed points. This value,

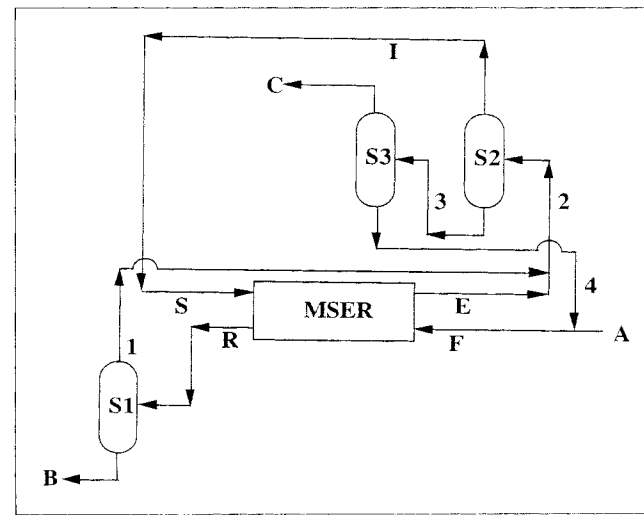

Figure 8. Process for improvement in yield (example 3).

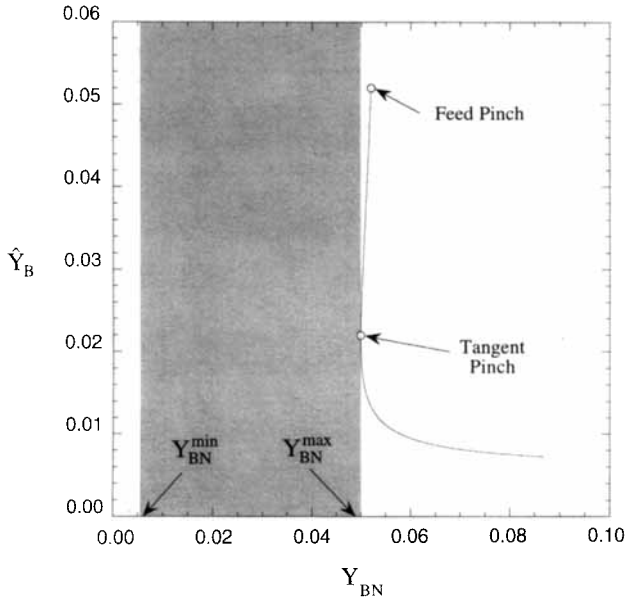

Figure 9. Fixed points and window of operation as a function of Y_{BN} for example 3 ($X_{B1} = 0.85$).

The shaded region indicates the feasible window of operation with the transformed mole fraction of component B in the extract stream leaving the final stage (Y_{BN}) being the key design variable.

Y_{BN}^{max}, corresponds to the upper limit on the window of operation. For $Y_{BN} \geq Y_{BN}^{max}$, the equilibrium and operating curves touch or intersect each other and the MSER operation is not feasible. The lower bound on the window of operation is the composition of the extract stream in equilibrium with the outlet raffinate stream, that is, Y_{B1}. Thus the window of operation of the MSER cascade is

$$Y_{B1} = Y_{BN}^{min} \leq Y_{BN} < Y_{BN}^{max}. \tag{66}$$

Within the window of operation the MSER profile attains the target composition in a finite number of stages. The window of operation is shown by the shaded region on Figure 9. The fixed point that controls Y_{BN}^{max} corresponds to a tangent pinch.

The trade-off between the number of stages and solvent flow within the window of operation is shown in Figure 10a for different specifications of X_{B1}. As expected, the stage requirement tends to infinity as we approach Y_{BN}^{max}. However, the solvent flow decreases as this limit is approached, thus reducing the size of each stage. Hence the optimal choice of Y_{BN} lies somewhere between the upper and the lower bounds. The yield of B goes through a maximum with increasing Y_{BN}, as shown in Figure 10b. For a given value of Y_{BN}, the yield of B increases with increasing X_{B1}. However, the stage requirement and solvent flow also increase. As can be seen from the phase diagram (Figure 2), Y_{B1} increases with decreasing X_{B1}. Hence in this case, as X_{B1} decreases, the window of operation shifts to the right and becomes narrower. In the limiting case of X_{B1} (and Y_{B1}) approaching the reactive plait point, both the upper and lower bounds on the window of operation coincide with the reactive plait point.

This design procedure can also be used to compare flowsheet alternatives. For example, for this process a flow sheet alternative where stream 1 is mixed with the solvent stream instead of the extract stream can also be used, as suggested by Samant and Ng (1998a). This alternative gives a slightly higher yield of B for any specification of R, X_{B1}, and Y_{BN}. However, the window of operation is very narrow and much higher solvent flows are required. Hence the flow sheet of Figure 8 is more attractive.

Example 4: Process for Improvement in Selectivity. Figure 11 shows a flow sheet for a process for improving the selectivity of the desired product of the system considered in Example 2. Samant and Ng (1998a) have shown that this flowsheet also has three degrees of freedom once the compositions of feed and product streams and the degrees of separations in the separators are specified. As before, the system can be

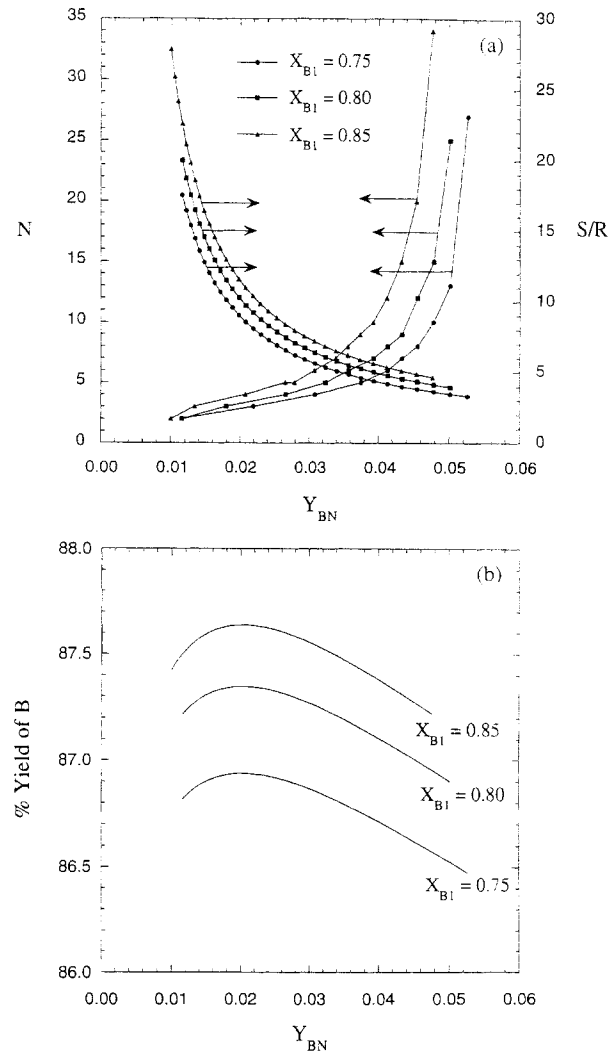

Figure 10. (a) Trade-off between equilibrium stage requirement and solvent flow for example 3; (b) yield of B as a function of Y_{BN} for example 3.

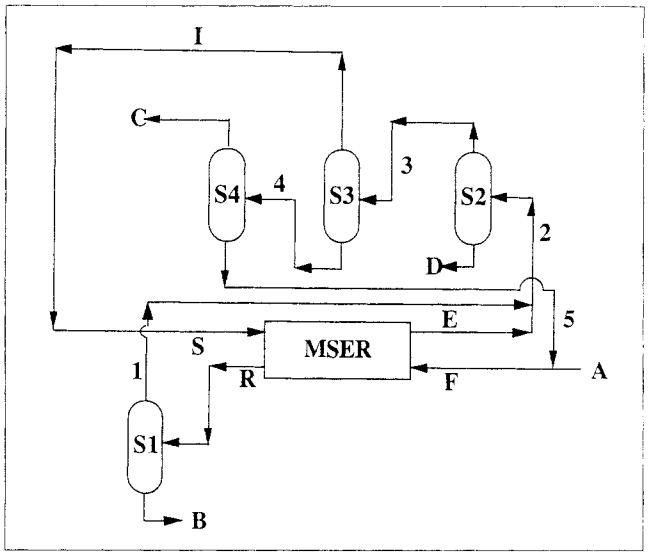

Figure 11. Process for improvement in selectivity (example 4).

completely specified by fixing R, X_{B1}, and Y_{BN}. Therefore, the formulation and solution of the fixed-point tracking problem is similar to the previous example.

Figure 12 shows the branch of fixed points (for $X_{B1} = 0.85$) that satisfy Eqs. 48, 49, and 65. This plot is also valid for any value of R. Here, again, we observe that there exists an upper bound on the window of operation. Here, the upper bound is controlled by the feed pinch and there are no tangent pinches in the MSER profile. The window of operation is shown by the shaded region on Figure 12.

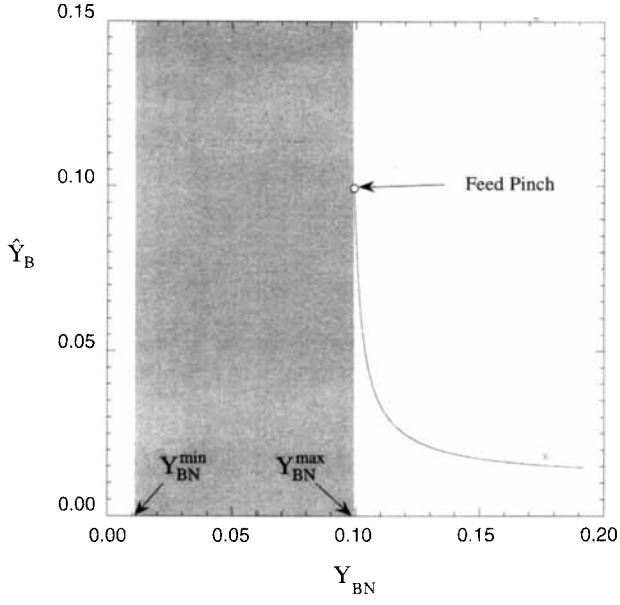

Figure 12. Fixed points and window of operation as a function of Y_{BN} for Example 4 ($X_{B1} = 0.85$).

The shaded region indicates the feasible window of operation with the transformed mole fraction of component B in the extract stream leaving the final stage (Y_{BN}) being the key design variable.

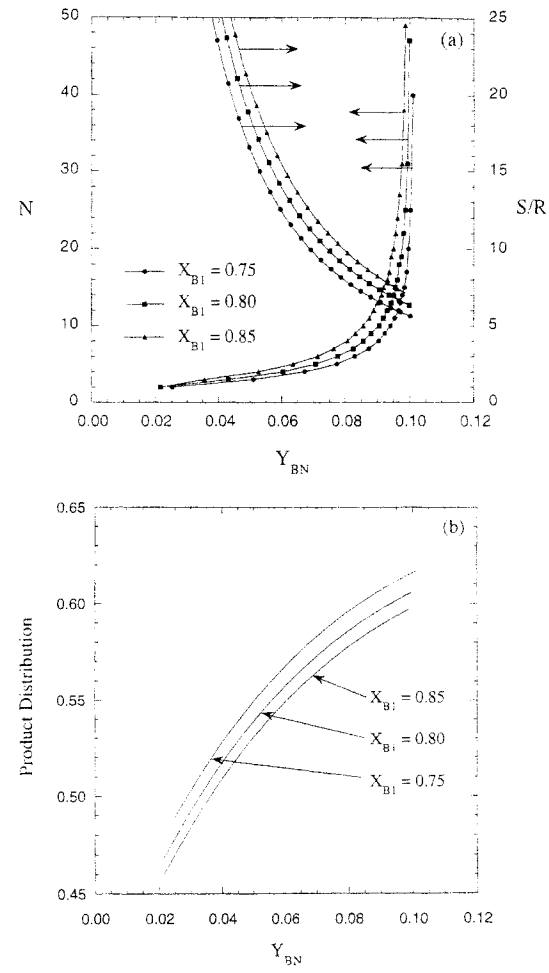

Figure 13. (a) Trade-off between equilibrium stage requirement and solvent flow for example 4; (b) product distribution as a function of Y_{BN} for example 4.

The trade-off between the number of stages and solvent flow within the window of operation is shown in Figure 13a for different specifications of X_{B1}. As before, the stage requirement increases and the solvent flow decreases as we approach Y_{BN}^{max}. Hence the optimal choice of Y_{BN} lies somewhere between the upper and the lower bounds. The product distribution increases with increasing Y_{BN} for all values of X_{B1}, as shown in Figure 13b. For a given value of Y_{BN}, the product distribution increases with decreasing X_{B1}. The stage requirement and solvent flow also decrease. As in the previous example, however, the window of operation becomes narrower and moves to the right as X_{B1} decreases until both the upper and the lower limits coincide with the reactive plait point when X_{B1} coincides with the reactive plait point.

Conclusions

Extractive reaction systems are multicomponent reactive systems with liquid–liquid phase separation. Such systems can

be obtained by deliberate addition of an immiscible liquid phase or can occur due to formation of products that are partially miscible with the reactants. Multistage processes involving extractive reactions can be synthesized to improve the yield or selectivity of a desired product or to facilitate separation of byproducts. The objectives of this article are to develop a calculation procedure for design of such multistage processes, to identify key design variables, and to assess their impact on process trade-offs.

The design procedure is generally applicable for systems with more than three components. Transformed mole fraction coordinates are used for the ease of visualization of the phase behavior of multicomponent systems. An important feature of the procedure is the analysis of the geometric properties of the MSER profiles. This analysis is carried out by tracking the fixed points or pinches of the MSER profile using arc-length continuation, and it determines the window of operation of the MSER. For design specification within the window of operation, the MSER profiles are feasible and the target composition is achieved in a finite number of stages. Once the window of operation is determined, the equilibrium stage requirements and process performance within this window can be easily determined. The fixed-point tracking does not require stage-to-stage calculations.

The procedure is illustrated with examples of the design of stand-alone MSER cascades and of MSER process flowsheets. In addition to providing information about process feasibility and performance, this procedure can also be used to help in screening flow-sheet alternatives for MSER processes. The analysis is limited to equilibrium-constrained systems, and it should be noted that slow reaction kinetics and mass transfer will influence the process performance. Effect of kinetics and mass-transfer on extractive reaction processes have been considered in a separate publication (Samant and Ng, 1998b).

Acknowledgment

The support of the National Science Foundation (grant No. 9807101) for this research is gratefully acknowledged. Additional support is provided by the National Environmental Technology Institute.

Notation

E_k, R_k = molar flow rates of extract and raffinate streams leaving stage k, mol/s
E_p, R_p = molar flow rates of extract and raffinate streams at the pinch, mol/s
$\hat{E}_p, \hat{R}_p$ = transformed molar flow rates of extract and raffinate streams at the pinch, mol/s
N = number of theoretical stages in the MSER cascade
p = number of phases
P = pressure, atm
T = temperature, K
x_i = mole fraction of component i
X_i = transformed mole fraction of component i
$\hat{Y}, \hat{X}$ = column vector of transformed mole fractions at the pinch in extract and raffinate streams, respectively
$\hat{Y}_i, \hat{X}_i$ = transformed mole fraction of component i at the pinch in extract and raffinate streams, respectively
y_{ik}, x_{ik} = mole fraction of component i in extract and raffinate streams leaving stage k
z_{iF}, z_{iS} = mole fraction of component i in feed and solvent streams, respectively
γ_i = activity coefficient of component i
$\nu_{\mathrm{TOT},m}$ = algebraic sum of the stoichiometric coefficients of the components in reaction m

Literature Cited

Anderson, W. K., and T. Veysoglu, "A Simple Procedure for the Epoxidation of Acid Sensitive Olefinic Compound with m-Chlorperbenzoic Acid in an Alkaline Biphasic Solvent System," *J. Org. Chem.*, **38**, 2267 (1973).
Berry, D. A., and K. M. Ng, "Synthesis of Reactive Crystallization Processes," *AIChE J.*, **43**, 1737 (1997).
Chapman, T. W., "Extraction—Metals Processing," *Handbook of Separation Process Technology*, R. W. Rousseau, ed., Wiley, New York (1987).
Coca, J., G. Adrio, C. Y. Jeng, and S. H. Langer, "Gas and Liquid Chromatographic Reactors," *Preparative and Production Scale Chromatography*, G. Ganestos and P. E. Barker, eds., Dekker, New York (1993).
DeGarmo, J. L., V. N. Parulekar, and V. Pinjala, "Consider Reactive Distillation," *Chem. Eng. Prog.*, **3**, 43 (1992).
Doherty, M. F., and G. Buzad, "Reactive Distillation by Design," *Trans. Inst. Chem. Eng.*, **70**, 448 (1992).
King, M. L., A. L. Forman, C. Orella, and S. H. Pines, "Extractive Hydrolysis for Pharmaceuticals," *Chem. Eng. Prog.*, **5**, 36 (1985).
Kubicek, M., "Algorithm 502 Dependence of Solution of Nonlinear Systems on a Parameter," *ACM Trans. Math. Softw.*, **2**, 98 (1976).
Kuntz, E. G., "Homogeneous Catalysis in Water," *Chemtech*, **9**, 570 (1987).
Mersmann, A., and M. Kind, "Chemical Engineering Aspects of Precipitation from Solution," *Chem. Eng. Tech.*, **11**, 264 (1988).
Minotti, M., M. F. Doherty, and M. F. Malone, "A Geometric Method for the Design of Liquid Extractors," *Ind. Eng. Chem. Res.*, **35**, 2672 (1996).
Pahari, P. K., and M. M. Sharma, "Recovery of Morpholine Via Reactive Extraction," *Ind. Eng. Chem. Res.*, **30**, 2015 (1991).
Samant, K. D., and K. M. Ng, "Synthesis of Extractive Reaction Processes," *AIChE J.*, **44**, 1363 (1998a).
Samant, K. D., and K. M. Ng, "Effect of Kinetics and Mass Transfer on Design of Extractive Reaction Processes," *AIChE J.*, **44**, 2212 (1998b).
Seader, J. D., "Computer Modeling of Chemical Processes," *AIChE Monog. Ser.*, Vol. **81**, No. 15 (1985).
Sharma, M. M., "Multiphase Reactions in the Manufacture of Fine Chemicals," *Chem. Eng. Sci.*, **43**, 1749 (1988).
Sorenson, J. M., and W. Arlt, "Liquid-Liquid Equilibrium Data Collection," *DECHEMA Chemistry Data Ser.*, Vol. 5, Parts 2 and 3, DECHEMA, Frankfurt (1979).
Tonkovich, A. L. Y., and R. W. Carr, "Modeling of the Simulated Countercurrent Moving-Bed Chromatographic Reactor Used for the Oxidative Coupling of Methane," *Chem. Eng. Sci.*, **49**, 4657 (1994).
Treybal, R. E., *Mass Transfer Operations*, 3rd ed., McGraw-Hill, New York (1981).
Tsotsis, T. T., A. M. Champagnie, R. G. Minet, and P. K. T. Liu, "Catalytic Membrane Reactors," *Computer Aided Design of Catalysts*, R. E. Becker and C. Pereira, eds., Dekker, New York (1993).
Ung, S., and M. F. Doherty, "Vapor-Liquid Phase Equilibrium in Systems with Multiple Chemical Reactions," *Chem. Eng. Sci.*, **50**, 23 (1995a).
Ung, S., and M. F. Doherty, "Synthesis of Reactive Distillation Systems with Multiple Equilibrium Chemical Reactions," *Ind. Eng. Chem. Res.*, **34**, 2555 (1995b).

Appendix: Equivalence of Parallel and Series Reaction Schemes of Example 2 at Thermodynamic Equilibrium

The parallel and series reaction schemes under consideration are as given in Eqs. 59 and 60. In both cases, we consider the same components A, B, C, D, and I. Hence the phase equilibrium equations are the same for both cases. In

addition, at reaction equilibrium, both cases satisfy the following equations:

$$K_1 = \frac{\gamma_B x_B \gamma_C x_C}{\gamma_A x_A} \tag{A1}$$

$$K_2 = \frac{\gamma_D x_D}{\gamma_A x_A} \tag{A2}$$

$$K_3 = \frac{K_2}{K_1} = \frac{\gamma_D x_D}{\gamma_B x_B \gamma_C x_C}. \tag{A3}$$

Note that the compositions and activity coefficients in the preceding equations are evaluated at equilibrium. K_1 and K_2 represent the reaction equilibrium constants for the parallel reaction scheme of Eq. 59, and K_1 and K_3 represent the reaction equilibrium constants for the series reaction scheme of Eq. 60. Thus, in both cases the reacting system satisfies the same set of equations at phase and reaction equilibrium. Hence, they are equivalent at thermodynamic equilibrium.

It should be noted that the behavior of the system in the preceding two cases will be quite different when far from thermodynamic equilibrium. This is due to the fact that the rate expressions and rate constants for series and parallel reactions are different. In other words, if we start with a certain initial composition, the system with reactions in series and the system with reactions in parallel would take different paths to the same composition at thermodynamic equilibrium. This situation is considered in more detail elsewhere (Samant and Ng, 1998b).

Manuscript received Jan. 23, 1998, and revision received July 15, 1998.